Solid base catalysts for pentaerythritol synthesis: Activity, stability, and recyclability of catalysts based on alkali and alkaline earth metals

Chemical Engineering Journal 543 (2026) 177975

Contents lists available at ScienceDirect

Chemical Engineering Journal

journal homepage: www.elsevier.com/locate/cej

Solid base catalysts for pentaerythritol synthesis: Activity, stability, and recyclability of catalysts based on alkali and alkaline earth metals

Aqsa Noreen [a], Abdenour Achour [a], Oleg Pajalic [b], Derek Creaser [a], Louise Olsson [a,*]

[a] Competence Center for Catalysis, Chemical Engineering, Chalmers University of Technology, SE 412 96, Gothenburg, Sweden
[b] Perstorp AB, Sweden

ARTICLE INFO

Keywords:
Pentaerythritol (penta)
Aldol condensation reaction
Cannizzaro reaction
Solid base catalyst
Formaldehyde
Acetaldehyde

ABSTRACT

The substitution of homogeneous bases with solid basic catalysts is highly desirable for the synthesis of pentaerythritol (penta), as liquid alkalis generate waste, accelerate reactor corrosion, and require extensive separation steps to isolate pure penta. This study investigates the catalytic activity of alkali and alkaline earth metals — Ca, Na, and Mg — supported on SnO_2, TiO_2, and γ-Al_2O_3 for the conversion of formaldehyde and acetaldehyde to penta. Reaction parameters including temperature, feed ratios, reaction time, and catalyst loading were examined to find optimized conditions to maximize penta selectivity. Among the tested systems, 22% Mg/γ-Al_2O_3 catalyst demonstrated the best performance, achieving 76% penta selectivity at 49% formaldehyde conversion under the following conditions: 90 °C, a 5:1 M ratio of formaldehyde to acetaldehyde, 0.2 g catalyst and 15 min reaction time. However, the leaching of Mg was siginficant. Mg on γ-Al_2O_3 with different Mg loadings were evaluated, showing that 9 wt% Mg/γ-Al_2O_3 catalyst exhibited the least amount of leaching, from 9 for fresh catalyst to 7.5 wt% Mg for spent catalyst (after reaction at 70 °C) and a penta selectivity of 61%, albeit at a slightly lower formaldehyde conversion of 41%. However, the accumulation of formate species on catalyst surface was observed with DRIFT spectroscopy, which resulted in deactivation of the catalyst. The catalyst partially regained the activity when recycled in multiple cycles after regeneration of spent catalyst. These findings highlight the potential of Mg-based solid catalysts for pentaerythritol synthesis, while also underscoring the need for further research to enhance catalyst stability and recyclability for industrial applications.

1. Introduction

To date, a wide range of valuable fine chemicals have been successfully produced from polyols through various routes namely catalytic, enzymatic, or fermentation [1–3]. Pentaerythritol (penta, $C_5H_8(OH)_4$) is a widely used polyol. It appears as a white, odorless crystalline solid, with a melting point of 260 °C and a boiling point of 276 °C. As a tetraol, penta is highly versatile: its neopentane backbone, bearing four hydroxyl groups on the terminal carbons, allows for substitution with a variety of functional groups or ions [4,5]. Due to its properties, penta is used to obtain important resins to produce plastics [6], polymers [7], cosmetics [8], oil additives [9,10], medicines [11], cross-linking agents [12], and various other commercial products [13,14].

Penta is generally produced when formaldehyde reacts with acetaldehyde with a strong alkaline base as a homogeneous catalyst under controlled conditions [15]. Four formaldehyde molecules react with one equivalent of acetaldehyde through the cross-aldol condensation and further reacting through a Cannizzaro reaction to give the final product penta. Alongside the desired penta production, the formation of undesired sodium formate salt by-product is occurring (Step 1, Scheme 1). Formates and methanol (MeOH) can also be produced from the self-Cannizzaro reaction of formaldehyde in the presence of a base as a catalyst.

Other hydroxylated by-products can also be formed, e.g. dipentaerythritol (dipenta), and hemiformals [16,17]. After completion of the reaction, the mixture is treated with an acid to neutralize residual alkaline hydroxides [18]. Following neutralization, the penta along with other hydroxylated by-products is subjected to drying to remove water from the mixture [19]. High-purity penta is then obtained through successive steps of crystallization, filtration, and decolorization [19–21]. Additional separation operations further contribute to water losses. As a result, penta manufacturing encounters two major challenges. The first is the generation of unwanted formate salts, which necessitates the use of excess formaldehyde. The second challenge lies in

* Corresponding author.
E-mail address: louise.olsson@chalmers.se (L. Olsson).

https://doi.org/10.1016/j.cej.2026.177975
Received 3 February 2026; Received in revised form 16 May 2026; Accepted 1 June 2026
Available online 25 June 2026

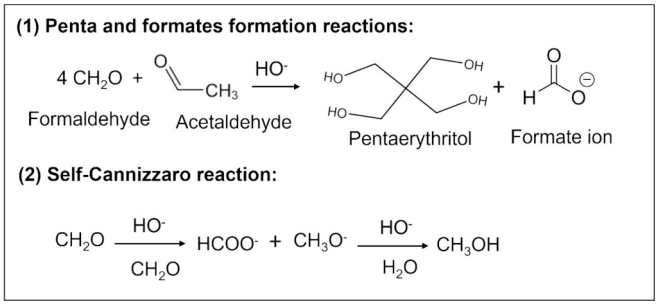

Scheme 1. Chemical reactions for the penta production and self-Cannizzaro reaction of formaldehyde.

that the process is very energy-intensive, largely due to the extensive separation required.

During the past several decades, research aimed at optimizing the penta synthesis process has remained limited. For example, Peters in 1955 investigated the effect of different operating parameters on penta yield losses [18]. It was reported that in experiments with sodium hydroxide as the liquid catalyst, the penta yield improved to 77% with an increase in temperature to 84 °C [18]. In 1957, Maury and co-workers patented an approach aimed at increasing penta yield by converting penta formals back into penta. This strategy involved adding an extra processing step in which penta formals dissolved in water were heated to temperatures between 150 and 300 °C in the presence of a cracking catalyst, such as composite silica–metal oxide catalysts [22]. To avoid the formation of by-products a continuous process was also introduced in 1965 by Greco et al. where acetaldehyde and NaOH were introduced during the reaction in multi-stage reactors in series. The authors claimed to obtain 87% yield based on acetaldehyde and 77% on formaldehyde [23]. There are several techniques introduced in patents to minimize losses by optimizing the operating parameters such as temperature, pH of the reaction mixture, the ratio between the formaldehyde, acetaldehyde, and alkali solution, reaction time, sequence of addition of reactants etc. Varying end product purities may be desired, i.e., monopenta of 98% purity or technical penta with 86–90% monopenta and 10–14% dipenta. However, several intensive separation steps are needed to achieve such a high yield which makes the process more expensive [24,25]. Belkin et al. in 2019 introduced a mathematical model to evaluate the efficiency of penta synthesis in reactors of various types and proposed a reaction mechanism based on the findings [26]. At present, mostly liquid alkali and alkaline earth homogeneous catalysts have been used to synthesize penta, due to their high activity towards aldol condensation and Cannizzaro reactions. However, several problems remain, such as liquid waste generated from homogeneous catalysts, the need to separate formates from the product stream and that the process is energy-intensive, largely due to the extensive separation required.

Heterogeneous catalysts, offer significant potential to overcome limitations associated with the use of liquid alkali and alkaline earth catalysts in various chemical syntheses. Several studies have demonstrated the effectiveness of solid base catalysts in promoting reactions such as aldol condensations and Cannizzaro reactions, typically in the context of synthesizing compounds like benzaldehyde derivatives, hydroxypivaldehyde and lactic acid [27–29].

Heterogeneous catalysts have large advantages with separation from the product mixture and also the possibilities of regeneration and re-use compared to homogeneous catalysts. However, there are according to our knowledge, only one study available for penta synthesis using heterogeneous catalysis. In the study by Trybula and Terelak, published in 1990 [30], ion-exchange resin was used as a catalyst, instead of the conventional liquid alkaline catalysts. However, regenerating the resin with NaOH, the formation of methanol, and the reduced selectivity for pentaerythritol (30% selectivity in outside grade Penta stream) remained significant challenges for the process [30].

Solid base catalysts offer several advantages in base-catalyzed industrial processes: they facilitate easier separation, avoid reactor corrosion, and help mitigate waste handling issues. Building on the advantages of heterogeneous catalysis, this study introduces a novel solid base catalyst system for penta synthesis, replacing the conventional liquid basic catalyst. For this purpose, alkali (Na) and alkaline earth metals (Mg, Ca) were impregnated onto SnO_2, TiO_2 and γ-Al_2O_3, and their catalytic performance was assessed for penta synthesis. Furthermore, the influence of key reaction parameters — such as temperature, catalyst loading, reaction time, and the formaldehyde-to-acetaldehyde ratio — on penta selectivity was investigated. Catalyst reusability tests revealed that with the appropriate regeneration of catalyst, partial activity of the catalyst was regained for penta formation reaction. The findings offer valuable insights for the development of a heterogeneous catalysts to produce penta with high yield and selectivity.

2. Experimental section

2.1. Chemicals and reagents

Acetaldehyde (anhydrous, ≥99.5%, GC, Sigma-Aldrich), formaldehyde (formalin 36.4–37.0%, <0.1%MeOH), pentaerythritol (>99%, Sigma-Aldrich), dipentaerythritol (>99%, Sigma-Aldrich), tripentaerythritol (technical grade, Sigma-Aldrich), 1-trimethylsilylimidazole (TMSI, >98%, Sigma-Aldrich), *N*,*N*-bis-trimethylsilyl-trifluoroacetamide (BSTFA, ≥98.5%, Sigma-Aldrich), pyridine (99%, Sigma-Aldrich), n-eicosane (C20, ≥99%, Sigma-Aldrich), 1,3,5-trioxane (≥99%, Sigma-Aldrich), titanium(IV) oxide (anatase, nanopowder, <25 nm particle size, 99.7%, Sigma-Aldrich), sodium nitrate (ACS reagent, ≥99.0%, Sigma-Aldrich), calcium nitrate tetrahydrate (crystalline, 99.98%, Alfa Aesar), magnesium acetate tetrahydrate (≥99%, Sigma-Aldrich), aluminum nitrate nonahydrate (≥98%, Sigma-Aldrich), aluminum oxide (gamma-phase, 99 + %, Alfa Aesar), tin(IV) oxide (nanopowder, ≤100 nm avg. part. size, Sigma-Aldrich), magnesium nitrate (>98%, Sigma-Aldrich), activated charcoal (Powder, Sigma-Aldrich), and deionized water were used in this work. Formaldehyde was stored in an oven at 45 °C to avoid solid formation due to its polymerization reaction at low temperatures. All chemicals were used without further pretreatment.

2.2. Catalysts

2.2.1. Catalyst preparation

Alkali and alkali earth metals (Na, Ca, and Mg) were supported on SnO_2, TiO_2, γ-Al_2O_3. These metals were impregnated onto the supports using wetness impregnation (WI) method, followed by ultrasonication for 30 min. Next, after subsequent drying overnight at 80 °C, calcination was done at 450 °C for 4 h after heating at a rate of 5 °C/min. Additionally, activated charcoal (AC) was used as a support precursor to prepare another variation of the Al_2O_3-supported catalyst. In this case, $Mg(NO_3)_2$ and $Al(NO_3)_3$ salts were mixed in a 10:90 wt% ratio and thoroughly kneaded onto the AC using a spatula. After drying overnight at 80 °C, the sample was calcined at two different temperatures of 500 °C and 750 °C for 4 h, with the heating rate of 8 °C/min. These samples were designated as Mg/Al_2O_3(AC_500°C)(12) and Mg/Al_2O_3(AC_750°C)(13), respectively.

2.3. Catalyst characterization

Specific surface areas and pore size parameters were determined by nitrogen adsorption–desorption analysis conducted at 77.4 K using a TriStar 3000 instrument. Prior to analysis, the samples were degassed at 120 °C for 3 h under a steady nitrogen flow. Surface area values, along with micro- and mesopore size distributions, were calculated using the BET and BJH methods.

Table 1
BET data of all fresh catalysts.

Catalyst	Mg or Na wt% loading based on ICP	S_{BET} (m^2/g)[a]	V (cm^3/g)[b]	Pore width (nm)
SnO_2	–	35.2	0.061	8.7
γ-Al_2O_3	–	149.6	0.515	11.4
TiO_2	–	103.8	0.357	10.9
Mg/SnO_2(30)	30	19.4	0.086	15.7
Mg/ γ-Al_2O_3(22)	22	53.3	0.192	10.6
Mg/TiO_2(24)	24	33.5	0.139	12.3
Na/SnO_2(18)	18	4.4	0.018	13.8
Na/ γ-Al_2O_3(27)	27	49.9	0.217	15.0
Na/TiO_2(23)	23	1.5	0.005	10.5
Mg/ γ-Al_2O_3(18)	18	55.9	0.235	13.4
Mg/ γ-Al_2O_3(9)	9	93.6	0.418	14.3

[a] S_{BET} (total surface area) calculated using the BET equation.
[b] V (total pore volume) calculated by single-point method at $P/P_0 = 0.95$.

X-ray diffraction (XRD) measurements of the prepared catalysts were performed using a Bruker D8 Advance powder diffractometer equipped with Ni-filtered Cu Kα radiation (λ = 0.15418 nm). The diffractometer was operated at 40 kV and 40 mA. Diffraction patterns were recorded over a 2θ range of 20° to 80°, with a scanning rate of 1° min^{-1} and a step interval of 0.02°.

CO_2 temperature-programmed desorption (CO_2-TPD) measurements were carried out using a digital scanning calorimeter (Sensys DSC, Setaram) equipped with a quartz sample holder and connected to a mass spectrometer (HPR-20 QUI, Hiden). Approximately 20–40 mg of catalyst was initially treated under an argon flow of 30 NmL min^{-1} at 300 °C for 30 min. Following this pretreatment step, the sample was cooled to 40 °C and saturated with a CO_2/Ar mixture containing 50 vol% CO_2 at a total flow rate of 30 NmL min^{-1} for 30 min. Excess and weakly adsorbed CO_2 was subsequently removed by purging with argon for 1 h. The TPD analysis was then conducted by heating the sample from 40 to 700 °C at a ramp rate of 10 °C/min under an argon atmosphere (30 NmL min^{-1}). The desorbed gases were monitored using mass spectrometry by tracking the $m/z = 44$ signal. Catalyst basicity was quantified from the total amount of CO_2 released during desorption.

NH_3-TPD analysis was performed on all the prepared catalysts and supports to determine the acidity of the samples using the same equipment as described for CO_2-TPD. About 20–40 mg of catalyst was pretreated by a flow of Ar (30 NmL/min) at 300 °C for 0.5 h. After the pretreatment, the catalyst was exposed to an NH_3-Ar mixture (1.0% NH_3 by volume, 30 NmL/min) at 100 °C for 2 h and then flushed with a flow of pure Ar (30 NmL/min) at the same temperature for 1 h to remove physisorbed NH_3, before cooling down the samples to room temperature. The samples were then heated from room temperature to 700 °C at a rate of 10 °C/min in a flow of Ar (30 NmL/min). The desorbed NH_3 was monitored using a mass spectrometer analyzing the mass number $m/z = 17$.

Elemental analysis of fresh and spent catalysts was conducted using the inductively coupled plasma sector field mass spectroscopy (ICP-SFMS) method, performed by ALS Scandinavia AB, Sweden. DRIFTS measurements were carried out on a Vertex 70 FT-IR spectrometer (Bruker) with an MCT detector and a diffuse reflectance accessory (Thermo Scientific™). Powdered samples were loaded into a high-temperature reaction cell (Harrick Praying Mantis) with a CaF_2 window. Temperature and gas flow were controlled using a Eurotherm 2416 controller and Bronkhorst mass flow controllers, respectively. Before the analysis, each sample was diluted with KBr and pretreated at 120 °C for 3 h, under 200 NmL/min Ar flow. After cooling down to 30 °C, the adsorption spectra were recorded. All the spectra were collected over 4000–1000 cm^{-1} with a resolution of 4 cm^{-1}. Thermogravimetric analysis of both fresh and spent catalysts was performed using a TGA/DSC 3+ (Mettler Toledo) instrument. Approximately 1–5 mg of each sample was placed in an aluminum crucible and heated from 30 to 600 °C with a ramping rate of 10 °C/min under an air flow of 100 NmL/min. Weight loss was observed across the temperature range of 100–600 °C. Derivative weight loss curves were calculated to identify the types of compounds decomposing at different temperatures.

2.4. Procedure for pentaerythritol synthesis

Formaldehyde was stored at 45 °C in an oven to avoid polymer formation. Before using formaldehyde in catalyst activity tests, Karl Fischer analysis was performed to quantify the water content and monitor the formaldehyde feed composition, which was 37% ± 2% in all experiments. All penta synthesis experiments were performed in batch reactor as a round bottom glass flask of 100 mL volume attached to a large glass double coil vertical cooling reflux condenser and a water bubble trap at room temperature. Continuous stirring was fixed for all the experiments at 200 rpm. Before testing the activity of the catalysts, blank reactions with formaldehyde and acetaldehyde, without catalyst, were performed to determine the losses of both the aldehydes at 70 and 90 °C in the experimental setup and to determine the reactivity of the reactants without a catalyst. All prepared catalysts listed in Table 1 (except pure supports) were initially tested under identical reaction conditions: a formaldehyde-to-acetaldehyde molar ratio of 5:1 (1 g acetaldehyde and 9.2 g of 37 wt% formaldehyde solution), 0.2 g of catalyst, a constant temperature of 70 °C, and a reaction time of 15 min. The mixture was then heated from room temperature to the reaction temperature, and the heating took about 15 min. Once the target reaction temperature was reached, the reaction time was set to zero. The best catalyst in terms of penta yield and selectivity among those screened at the initial conditions was further examined for its performance under varying conditions including formaldehyde-to-acetaldehyde initial molar ratios, catalyst loadings, temperatures, and reaction times. To evaluate the influence of individual parameters, each condition was varied independently. The reaction temperature was examined in the range of 30–90 °C. Heating to 30 and 70 °C were achieved in 15 min, while 90 °C was reached in 20 min. Catalyst loading from 0.1 to 1 g, formaldehyde-to-acetaldehyde molar ratio from 3:1 to 7:1, and reaction time from 0 to 60 min, were evaluated.

After completing the reaction and cooling the reaction mixture to room temperature, the catalyst was separated from the liquid by vacuum filtration. The recovered solid catalyst was then dried in an oven at 90 °C for 2 h. The spent catalysts were regenerated by calcination at 450 °C for 1 h. These regenerated catalysts were used in recycling tests for penta formation, under the same reaction conditions as discussed above (for fresh catalyst). The same product separation protocol was used for the products obtained from each catalyst recycling test. Non-regenerated spent catalyst was also recycled to check its activity for the penta formation reaction.

2.5. Product analysis

Gas chromatography–mass spectrometry (GC–MS) was utilized for the qualitative analysis of residual reactants and reaction products. Detailed analytical conditions are provided in the Supplementary information (SI). An aliquot of the liquid filtrate was directly injected into GC vials for the determination of unconverted formaldehyde, acetaldehyde, and other low-molecular-weight compounds. 1,3,5-Trioxane (10,000 ppm) was employed as an internal standard. Quantification of penta and its derivatives was achieved using a silylation-based derivatization procedure, as described in the SI Section S1.

2.6. Data processing

The formaldehyde conversion, product selectivities and carbon recovery were calculated according to Eqs. (1)–(3), respectively:

$$\text{Formaldehyde Conversion (mol\%)} = \frac{\text{mole of formaldehyde converted}}{\text{mole of initial formaldehyde}} \times 100 \quad (1)$$

$$\text{Product Selectivity (mol\%)} = \frac{\text{n x (mole of product)}}{\text{mole of formaldehyde converted}} \times 100 \quad (2)$$

$$\text{Carbon recovery} = \frac{\text{Total moles carbon: (detected products and reactants) + (formates produced) + (experimental losses)}}{\text{(total moles of initial carbon in reactants)}} \times 100 \quad (3)$$

In Eq. (2), n represents the stoichiometric number of moles of formaldehyde required to produce one mole of the product. The n value for each specific product was determined based on its chemical structure and formation mechanism. For penta, the n was set to 4, reflecting its formation via three aldol reactions and one Cannizzaro reaction involving formaldehyde. For penta-derivatives, mainly consisting of cyclic penta, dipenta, and linear monoformal penta as identified by GC–MS analysis, the corresponding n values were 5, 8, and 9, respectively, according to their structural characteristics. For diol (1,4-butenediol), n was assigned a value of 2, as it forms through condensation reactions of formaldehyde and acetaldehyde.

Product selectivity was calculated based on the amount of formaldehyde converted, as significant losses of acetaldehyde occurred (trapped in water bubbler) during the experiments due to its high volatility. In a blank experiment conducted at 70 °C, under typical reaction conditions, 12 wt% of acetaldehyde and 2 wt% of formaldehyde were lost. At 90 °C, the acetaldehyde loss increased to 62%, while formaldehyde losses reached 4 wt%. Due to these substantial losses, acetaldehyde conversion could not be accurately quantified and carries greater uncertainty compared to formaldehyde. The minor losses observed experimentally for formaldehyde were accounted for in the calculations of formaldehyde conversion, product selectivity and carbon recovery.

The total moles of carbon in all products and remaining reactants were summed to calculate the carbon recovery. It was assumed that one mole of formate was produced for each mole of penta formed, as well as for each mole of penta needed to produce any penta-derivative products (cyclic and linear forms of penta, and dipenta). These estimated formate quantities were included in the carbon recovery calculation (Eq. (3)) and are reported in the Supplementary information as carbon balance for each experiment. Thus, no direct measurements were performed to quantify formates produced. Moreover, it is important to note that formaldehyde is consumed in the formation of penta, penta-derivatives (linear, and cyclic form of penta, dipenta), diols (1,4-butenediol), and formates. A complete spectrum of the liquid product mixture is shown in Fig. S1b, Supplementary information (SI). Overall, carbon recovery ranged from 85% to 116%, with discrepancies from 100% explained by analytical limitations and the complexity of quantifying minor pentaerythritol-derived species. The deviation in carbon balance can possibly cause the over-estimation or under-estimation of the reported values of selectivity and conversions.

The sum of the product selectivities in all cases ranged from 91 to 103%, calculated based on the experimentally measured formaldehyde conversion (Eq. (2)), which is in the range of experimental accuracies.

The leaching was determined according to the following equation:

$$\text{Leaching (percentage points)} = (\text{wt.\%of basic metal in fresh catalyst} - \text{wt.\%of basic metal in spent catalyst} * f_{dilution}) \quad (4)$$

where the dilution factor, $f_{dilution}$, is added to compensate for any residual products or formates in the solids for spent catalyst. This factor is derived from the measurement of the amount of Al, Ti or Sn in the support.

$$f_{dilution} = (\text{wt.\%of Al, or Ti or Sn in Fresh catalyst})/(\text{wt.\%of Al, or Ti or Sn in Spent catalyst}) \quad (5)$$

3. Results and discussions

3.1. Catalyst characterization

ICP analysis was performed on all the prepared catalysts, and the data is shown in Tables 1 and S1 (SI). The pore structure results for all the supports and alkaline earth/alkali-metal impregnated catalysts are shown in Fig. 1 and Table 1. Among the supports, γ-Al_2O_3 has a higher surface area and porosity compared to TiO_2 and SnO_2 (Fig. 1a). Generally, impregnating Na and Mg on all supports led to a decrease in surface area and specific pore volume except for Mg/SnO_2 where the pore volume increased compared to SnO_2. The results shown in the table and pore size distribution curves indicate that impregnating Na on alumina led to the blockage of mainly small pores, leading to an increased average pore size. This was also the case for two of the Mg based catalysts (Table 1 and Fig. 1), as also reported in the literature [31]. Among the three supports, pore width changes due to metal loadings were small for TiO_2. Moreover, surface areas were lower for samples with higher Mg loadings (Figs. 1d, S2 and Table 1), which is expected since higher loading results in more blockage.

SEM analysis of the freshly prepared Mg/γ-Al_2O_3(22) catalyst, as well as the γ-Al_2O_3 support were performed to examine its morphology (Figs. S3 and S4). Fig. 2 shows the XRD patterns of the supports and metal-impregnated catalyst samples. In the prepared catalyst samples, the XRD peaks for the supports SnO_2, and TiO_2 can be observed. However, the intensity of the peaks for the γ-Al_2O_3 is weak due to a more amorphous structure (Fig. 2a). For Mg-based catalysts, a clear peak close to 43° for MgO was observed and not present for the pure supports. Moreover, with increasing loadings of Mg on γ-Al_2O_3 (Fig. 2b), the intensity of MgO increased. The average crystallite size was also calculated for these catalysts using the Scherrer equation based on the XRD data. The details about the calculation and average crystallite sizes can be found in Table S2 (SI). Overall, it was observed that the Na-based

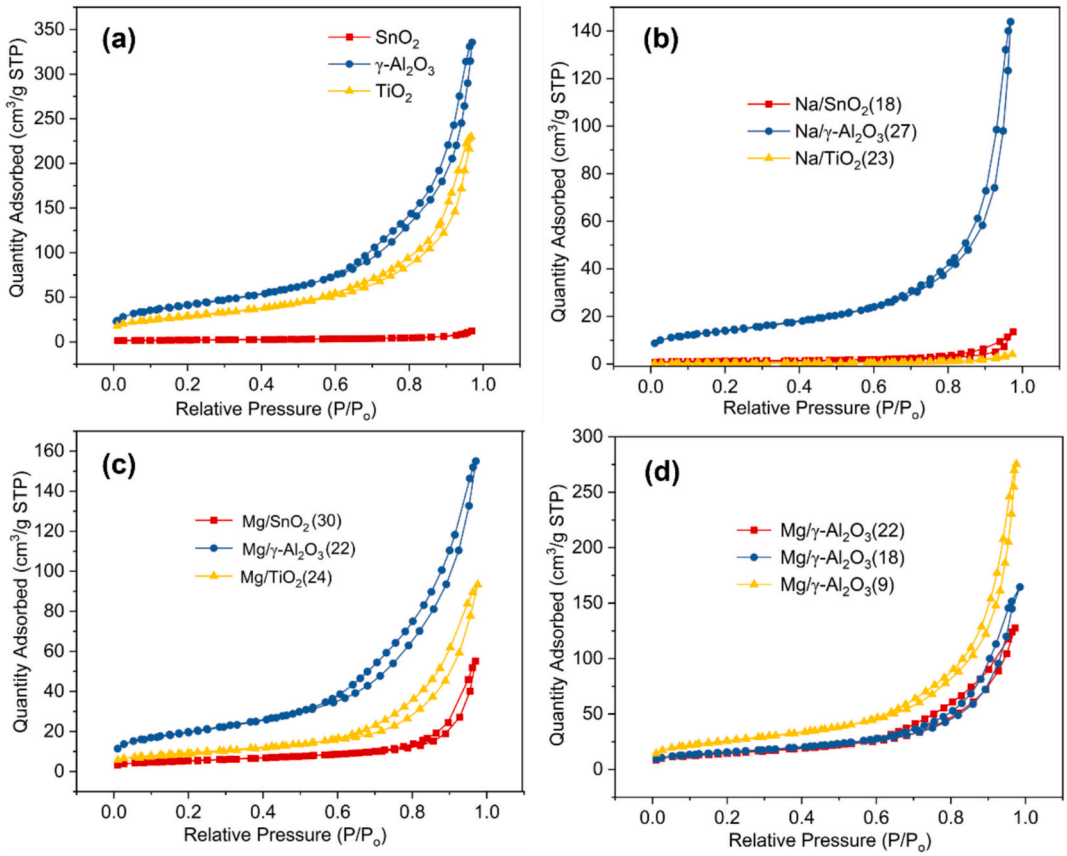

Fig. 1. N_2 physisorption isotherms for (a) supports, (b) Na based catalysts with different supports, (c) Mg based catalysts with different supports, (d) Mg based catalysts with different Mg loadings on γ-Al_2O_3.

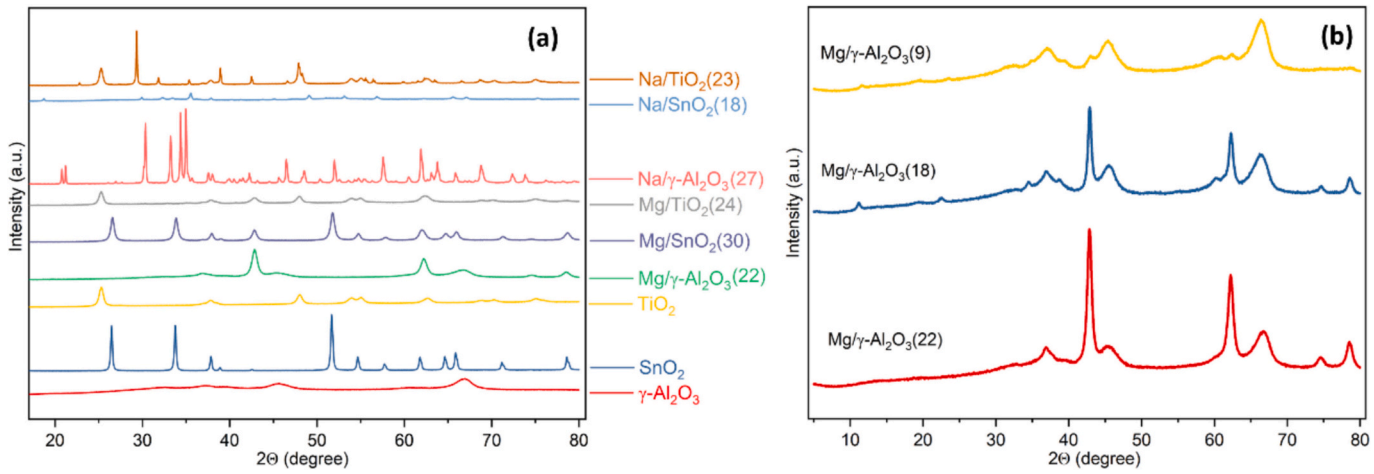

Fig. 2. XRD analysis of (a) supports, Na and Mg-based catalysts on different supports, (b) Mg-based catalysts with different Mg loading on γ-Al_2O_3.

supported catalysts have larger average crystallite sizes (based on all the major peaks present in the XRD scans). This is possibly due to the strong Mg^{2+} ions interaction with the support's surface O^{2-} resulting in a higher dispersion of Mg. In addition it is possible that Mg partially incorporates in the crystal and forms mixed oxides [32]. On the other hand, Na^{+} likely has weaker interactions with the surface. Moreover, among the Mg/γ-Al_2O_3 catalysts, when decreasing the loadings of Mg, the average crystal size decreases from 10.4 to 3.8 nm for Mg/γ-Al_2O_3(22) and Mg/γ-Al_2O_3(9) (see Table S2). Different crystallite sizes of Na and Mg might impact their activity towards penta formation, as well as their stability.

The CO_2-TPD analysis was performed to evaluate the basicity of the prepared catalysts. The CO_2-TPD curves for all supports and prepared catalysts are shown in Fig. 3. The basicity of the catalysts is expected to significantly influence their catalytic performance. The distribution of basic sites classified as weak, medium, and strong, and are here assigned to the CO_2 desorption peaks in the temperature ranges of 100–200 °C, 200–500 °C, and above 500 °C, respectively [33]. The weak basic sites can be associated with the OH-groups on the surface, the medium strength can be assigned to the oxygen attached to both impregnated metals and support metals, and strong basic sites to the low-coordination surface of the isolated O^{2-} anions [33]. In general, among the supports,

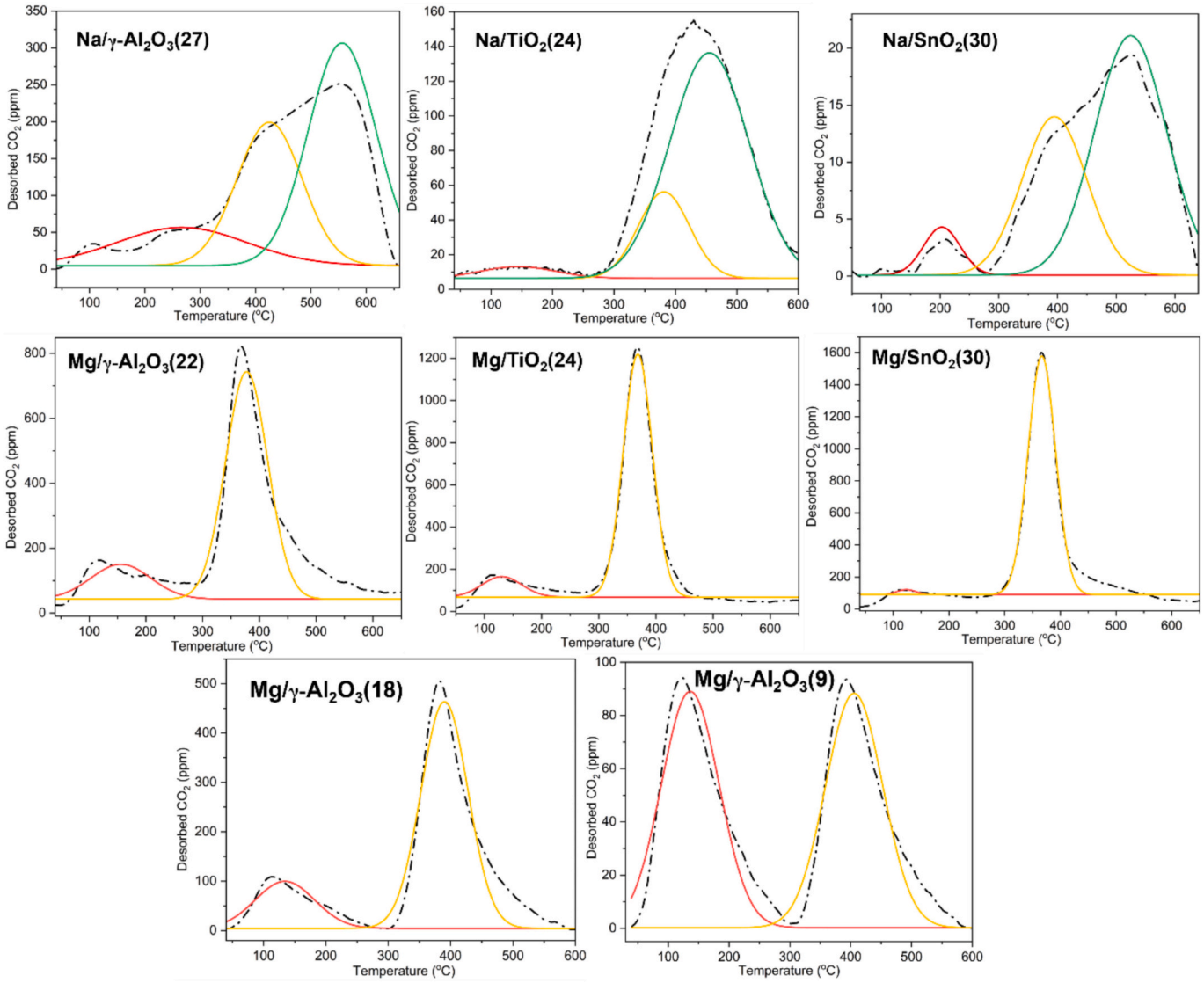

Fig. 3. CO_2 TPD curves of Na based catalysts, Mg based catalysts, and various loadings of Mg on γ-Al_2O_3 support.

Table 2
CO_2 adsorption capacity (μmol/g catalyst) indicating the basic strength of all prepared catalysts and supports.

Catalyst	Total basicity μmol/(g catalyst)	Basic sites distribution (%)		
		Weak	Medium	Strong
Mg/γ-Al_2O_3(22)	410	18	82	0
Mg/TiO_2(24)	422	10	90	0
Mg/SnO_2(30)	515	1	85	14
Na/γ-Al_2O_3(27)	163	17	32	51
Na/SnO_2(18)	51	6	35	59
Na/TiO_2(23)	112	4	19	77
γ-Al_2O_3	59	100	0	0
TiO_2	Undetected	–	–	–
SnO_2	Undetected	–	–	–
Mg/γ-Al_2O_3(18)	366	21	79	0
Mg/γ-Al_2O_3(9)	152	51	49	0

γ-Al_2O_3 exhibits a greater number of weak basic sites compared to the TiO_2 and SnO_2 (Table 2). Alkali and alkaline earth metals impregnated onto the support enhanced the abundance of basic sites, especially those with medium (200–500 °C) and strong (above 500 °C) basic strengths. The desorption between 100 and 200 °C on bare γ-Al_2O_3 was 59 (μmol/g), while Mg/γ-Al_2O_3(22) exhibited 74 μmol/g, showing that also the Mg contributed to weak acid sites. The distribution of basic sites varied among all the supported catalysts. Table 2 shows that Mg-based catalysts have a larger amount of CO_2 desorbed per gram of catalyst compared to the Na-based catalysts. In addition, both impregnated catalysts have different types of basic sites. Mg-based catalysts have predominantly medium basic sites in the temperature range of 300–450 °C (82–90% of total basicity), see Fig. 3 and Table 2. These results indicate the presence of $Mg^{2+} - O^{2-}$ pairs on the surface. While on the other hand, Na-based catalysts have both medium and strong basic sites, mostly in the 300 to 600 °C temperature range (Fig. 3). This could be due to the ability for Na to donate electrons and that low coordinated O^{2-} serve as basic sites on the catalyst surface [34].

Among the Na-based catalysts, Na/γ-Al_2O_3(27) exhibits an intense peak with the highest amount of total basic sites (163 μmol/g, Fig. 3 and Table 2), which might be due to the larger dispersion of Na on the γ-Al_2O_3 support, providing more surface area compared to the other supports (Fig. 1b and Table 1). It is expected that the dispersion of Na would be higher on γ-Al_2O_3, since the surface area of γ-Al_2O_3 is significantly higher than for the other supports and this is also observed. However, this trend was not clear for the Mg based catalysts. The TPD curve for Mg/SnO_2(30) exhibited highest of medium basic sites (437 μmol/g) compared to the other Mg based catalysts (Table 2). Moreover, surface -OH were observed during the DRIFT analysis of Mg based

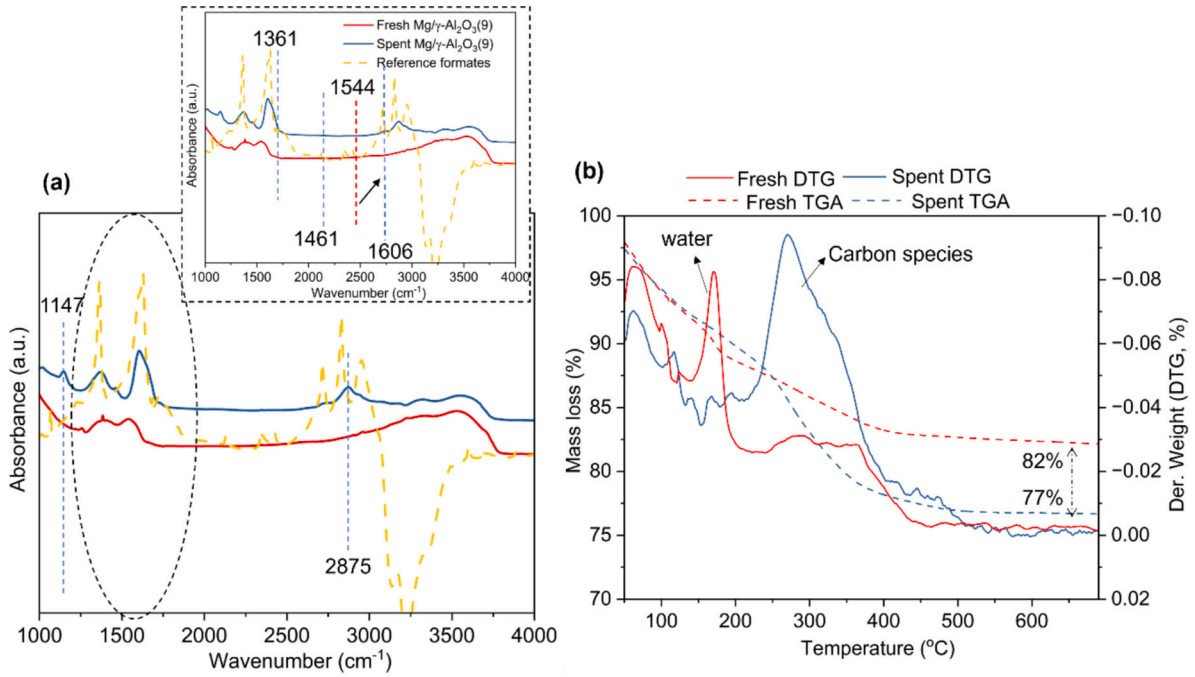

Fig. 4. Thermogravimetric and DRIFT analysis results for fresh and spent Mg/γ-Al_2O_3(9) catalyst, compared to Na-formate reference sample; (a) DRIFT spectra, and (b) TGA and DTG curves.

catalyst as shown in Fig. S5, which indicate that the surface -OH are serving as weak basic sites in these catalysts. On the other hand, these bands can also be due to surface moisture. Additionally, basicity decreases with reduced loading of Mg on the γ-Al_2O_3 support, as shown in Fig. 3 and Table 2. The different alkalinity of the catalysts and their respective distinctive desorption of CO_2 could affect their catalytic performance for penta synthesis.

The acidity of the bare supports and Mg-based catalysts was also determined based on the NH_3 TPD signals and the total acidity is reported in Table S2. Among the selected supports, γ-Al_2O_3 shows the total acidity of 191 μmol/(g cat), which was higher than all the other supports and Mg-based catalysts. As the Mg loading increases, a clear decrease in acidity was observed for Mg/γ-Al_2O_3(9), Mg/γ-Al_2O_3(18) and Mg/γ-Al_2O_3(22) catalysts compared to the bare support as shown in Table S2.

The DRIFT spectra and the thermogravimetric analysis results are shown in Fig. 4 for both the fresh and spent Mg/γ-Al_2O_3(9) catalysts. The DRIFT experiments were performed with samples diluted with KBr to enhance peak resolution and the spectra. The results shown in Fig. 4a, were obtained after pretreatment by heating to 120 °C for 3 h. In the DRIFT spectra, a broad band was observed in the 3200–3700 cm^{-1} range, corresponding to the O—H stretching vibrations of water molecules present in the samples. A weak band in the spent catalyst at 2875 cm^{-1} is attributed to strongly hydrogen-bonded water interacting with carbonaceous species such as formates [35]. Reference measurements on sodium formate, clearly shows formates in this region. Interestingly, in the lower wavenumber region, a clear peak between 1570 and 1700 cm^{-1} is observed in the spent catalyst, which is shifted to a higher wavenumber compared to the fresh catalyst's peak at 1544 cm^{-1}. This shift, clarified in the enlargement inset of Fig. 4a, suggests a difference in the nature of the carbonaceous species; carbonates are predominant in the fresh catalyst, while formates — formed as by-products of the Cannizzaro reaction — are deposited on the surface of the spent catalyst. Within the 1500–1700 cm^{-1} range, various formate species can be formed and are reported in the literature [36]. It is also evident that the spent catalyst exhibits peaks at around 1361 cm^{-1} and 1606 cm^{-1}, which closely match those of the Na formate reference sample, further supporting the presence of formates on the catalyst surface.

The thermogravimetric analysis (TGA) results for both the fresh and spent catalysts are shown in Fig. 4b. The fresh sample, analyzed without any pretreatment, exhibits a total weight loss of around 18%, which could be due to moisture and water trapped within the catalyst pores along with a small amount of surface carbonates, as indicated by the DTG curve. In contrast, the spent catalyst shows a broad peak at a higher temperature (200–400 °C), which likely corresponds to carbonaceous material decomposition. The spent catalyst exhibited a significantly higher weight loss of 33%, compared to 18% for the fresh sample. The larger mass loss from the spent catalyst is likely due to the presence of formates, in agreement with the DRIFTs results (Fig. 4a) and likely also some solid penta compounds retained in the catalyst after filtration of the reaction mixture.

3.2. Catalytic activities for penta synthesis reaction

3.2.1. Comparison of different solid catalysts

A catalyst-free control experiment reacting formaldehyde (37% in water) and acetaldehyde was performed at 70 °C with a formaldehyde to acetaldehyde feed ratio of 5:1 (molar). Samples were taken from 0 h to 1 h reaction time, and no other compounds were detected by GC–MS analysis except the reactants and traces of acetaldehyde self-condensation products (Fig. S6). All the prepared catalysts were thereafter examined under the same reaction conditions as in the control experiment, using formaldehyde containing a negligible amount of MeOH (<0.1 wt% MeOH as shown in Fig. S1c) as a reactant. An exception was made for one experiment, in which fresh formaldehyde with 10 wt% MeOH was used in the presence of the Na/TiO_2(23) catalyst. The product distribution in this case can be seen in Fig. S1a. Numerous by-products were found alongside the penta peak, likely due to the abundant formation of active enolate species in the presence of MeOH, which promotes multiple condensation and coupling reactions [37]. In contrast, experiments using formaldehyde with <0.1 wt% MeOH showed minimal cross-condensation products in the chromatogram (Fig. S1b).

The activities of different alkali and alkaline earth metals, i.e. Mg, Ca, and Na having different base properties were evaluated on three different supports: TiO_2, SnO_2, and γ-Al_2O_3 for penta synthesis. These

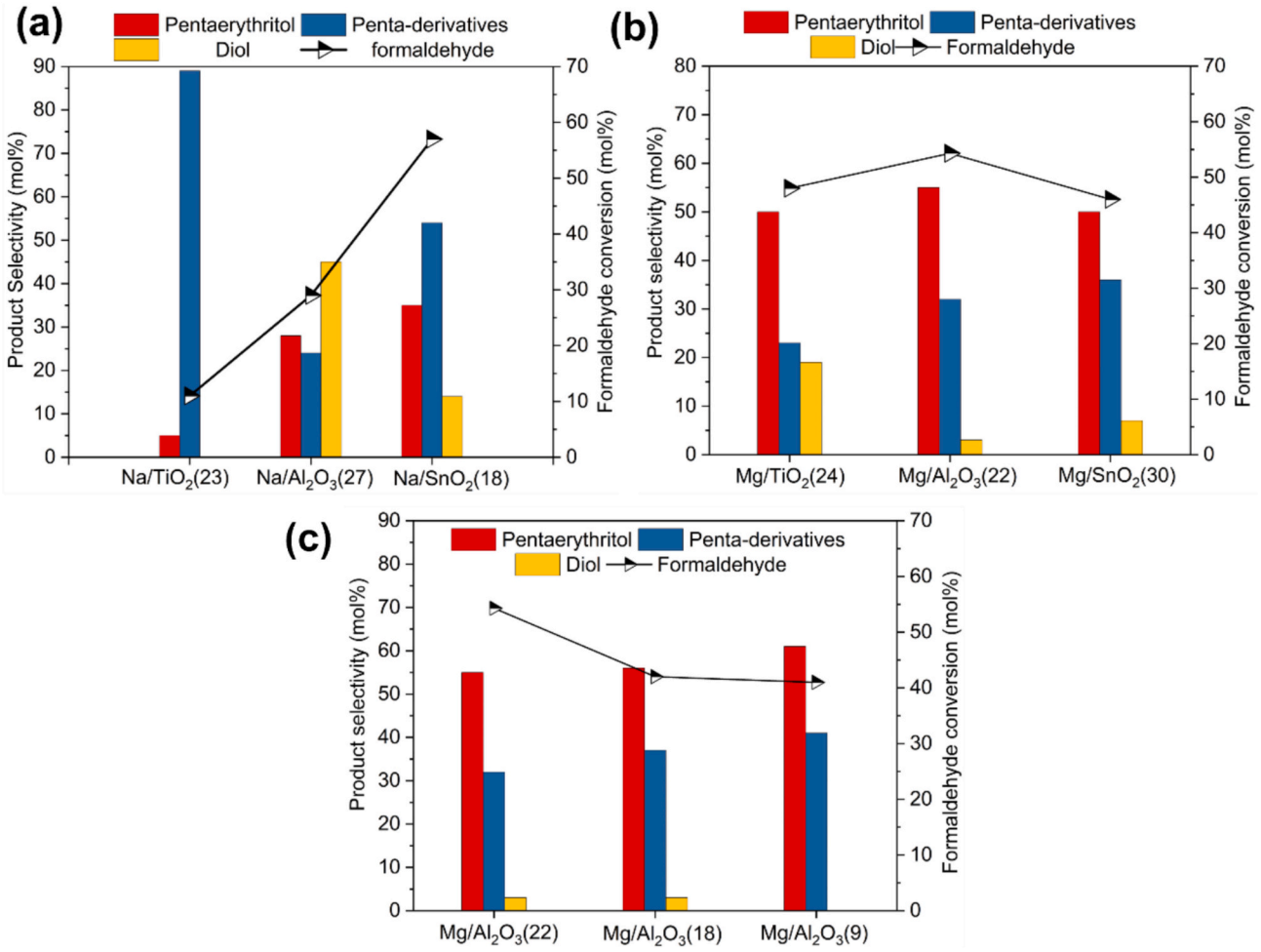

Fig. 5. Alkali and alkaline earth metals on various supports for penta synthesis showing (a) Na-based catalysts with different supports, (b) Mg-based catalysts with different supports, and (c) varying Mg loading on γ-Al_2O_3. Reaction conditions: formaldehyde to acetaldehyde feed ratio 5:1 (molar), 15 min reaction time, 70 °C temperature and catalyst amount of 0.2 g. It should be noted that the losses of formaldehyde in blank experiment conducted at 70 °C was 2%, while for acetaldehyde it was 12%. Mg/Al_2O_3 (9) catalyst activity tests were repeated three times, see Table S5.

supports have different surface areas, pore structures and acid/base properties that influence the impregnated catalyst activity performance and stability as discussed below. Notably, no self-condensation product (MeOH) was detected in the presence of these catalysts (Figs. 5a, S1b and Table S3). Among the alkaline earth metals, the Ca-based catalyst (Ca/SnO_2(28)) exhibited the lowest activity, with reduced conversion and penta selectivity (Table S4). Additionally, the Ca-based catalyst showed poor stability. After accounting for the dilution factor of 1.8 in spent catalyst, the Ca content decreased from 28 wt% in the fresh catalyst to 19.5 wt% in the spent sample, representing a loss of 8.5 percentage points. In contrast, both Na and Mg exhibited promising performance for penta synthesis.

Fig. 5 shows the catalytic behavior of the Na- and Mg-based catalysts, revealing distinct differences in the selectivity for the penta reaction. These differences can be attributed to basic/acid sites and type of the basic sites present in these catalysts. Na catalysts exhibited different behavior depending on the support, although all Na based samples contained strong basic sites. Thus, alkalinity is not the only property influencing the penta selectivity among Na-based catalysts. In detail, Na/TiO_2(23) showed low conversion of formaldehyde and mainly produced penta derivatives (Fig. 5a). On the other hand, Na/γ-Al_2O_3(27) achieved higher formaldehyde conversion (29%) and favored diol formation (45% selectivity), with 28% penta selectivity. However, Na/SnO_2(18) showed the highest activity among Na-based catalysts, with 57% formaldehyde conversion and selectivity of 35% for penta and 54% for penta-derivatives (Fig. 5a and Table S3).

Mg-based catalysts outperformed Na-based catalysts in both formaldehyde conversion and penta selectivity (Fig. 5a versus b). This performance of Mg-based catalysts might be linked to the absence of strong basic sites in Mg-based catalysts in comparison to Na-based catalysts (Table 2). The strong basic sites in the Na-based catalysts, such as O^{2-}, can likely produce reactive enolate from acetaldehyde. However, in case of Mg-based catalyst, Mg is not as reactive as Na and can possibly form a more stable enolate that leads to a better control of reaction which consequently reduces derivative formation. Specifically, Mg/γ-Al_2O_3(22) showed the highest penta selectivity of 55% among Mg-based catalysts (Table S3). It also exhibited the lowest diol selectivity, where especially Mg/TiO_2(24) exhibited large diol formation. The reduced by-product formation with Mg/γ-Al_2O_3(22) could possibly be linked to its lower amount of medium and strong basic sites compared to the other two Mg-based catalysts (Fig. 3 and Table 2). Moreover, lowering the Mg loading influenced the product distribution, mainly reducing the diol (1,4-butendiol) formation (Fig. 5c) and lowering the formaldehyde conversion. With Mg/γ-Al_2O_3(9), penta selectivity was 61% with no diol formation, although formaldehyde conversion dropped to 41%, as shown in Fig. 5c.

Reproducibility of this catalyst was also investigated, and catalytic activity tests were repeated 3 times for the Mg/γ-Al_2O_3(9) catalyst, and

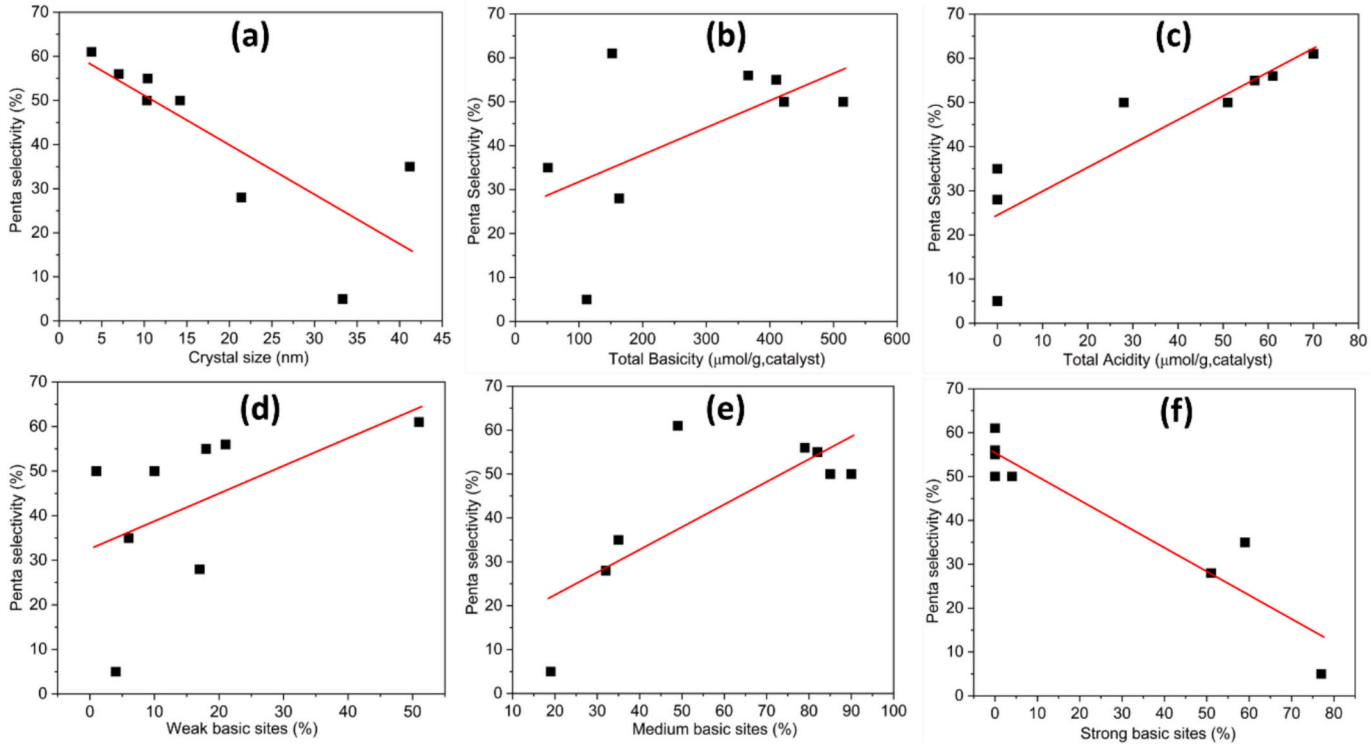

Fig. 6. Penta selectivity as parameter of catalyst performance in relation with (a) average crystallite sizes, (b) total basicity (μmol/g, catalysts), (c) total acidity (μmol/g, catalysts), (d) weak basic sites, (e) medium basic sites, and (f) strong basic sites of all the prepared catalysts. Symbols present the data points of different catalysts and solid lines indicate the trend line.

standard deviation values (S.D.) for conversion and selectivity are shown in Table S5. In Table S5, the 3rd repeated experiment was performed with another batch of prepared catalyst (Mg/γ-Al_2O_3) and the results are similarly with the old batch which show the reproducibility of the catalyst synthesis.

In order to further connect the penta formation with the structural properties of the catalyst, the penta selectivity is plotted versus different parameters (Fig. 6). The results show that penta selectivity is favored in general by: (i) small solid catalyst particles, (ii) high total basicity and (iii) high total acidity. In Fig. 6d to f the effect of different basic strength is shown, and it is clear that a large amount of medium strong sites is beneficial, but that strong basic sites are negative.

Moreover, catalysts derived from AC precursors performed poorly, favoring diol formation with lower formaldehyde conversion compared to the other Mg-based catalysts. Discussion relating to those results can be found in SI Section S4.

Catalyst stability was assessed by measuring the metal loadings in all spent catalysts by ICP analysis. The leaching results, reported in terms of the percentage points (see Eqs. (4)–(5)), are shown in Fig. S7a. Generally, Na-based catalysts exhibited significant leaching, ranging from 9.2 to 15.2 percentage points, whereas Mg-based catalysts showed much lower leaching, between 3.9 and 7.2 percentage points (Fig. S7a). Among them, Mg/γ-Al_2O_3(22) demonstrated quite high stability, with 4 percentage points Mg leaching, from 21.45 wt% in fresh catalyst to 17.4 wt% in spent catalyst (after accounting for the dilution factor of 2 in spent catalyst), while also achieving superior penta selectivity, as discussed earlier. Mg ions were strongly bound to the γ-Al_2O_3 support due to its acidic nature [38], resulting in more stable performance during penta formation compared to the other supported catalysts. Moreover, Mg leaching further decreased to 2.4 and 1.5 percentage points for catalysts Mg/γ-Al_2O_3(18) and Mg/γ-Al_2O_3(9) (Fig. S7a). This can be explained by the lower Mg loading of the Mg/γ-Al_2O_3(9). It should be noted that the loss in wt% is similar for all three catalysts (around 13–18 wt%).

According to the penta formation reaction, formaldehyde reacts with acetaldehyde in the presence of a base through three sequential steps of Aldol condensation, followed by the Cannizzaro reaction requiring an additional formaldehyde, yielding the final product, penta, along with alkali metal formate as a side product [18]. Theoretically, in the reaction pathway for penta formation, there is one mole formates produced when four formaldehydes are consumed to produce one penta, thus the ratio is 1:4 (0.25), as shown in Scheme 1. Since the solid catalysts examined in this study leach alkali/alkaline earth metals, it is plausible that the leached species act as homogeneous catalysts, particularly facilitating the Cannizaro reaction and leading to the formation of metal formates. The leached metal could undergo a homogeneous reaction to form metal formates, such as sodium formates. To investigate this possibility, we assume that all leached metal atoms form formates and divide that with the formaldehyde consumed for producing penta and penta derivatives, and the results are shown in Fig. S7b. Theoretically, the amount should be 0.25 (1:4 ratio) if all penta is produced via homogeneous catalyst path. The results in Fig. S7b show that for Na/TiO_2(23), the ratio is 0.05, and since this value is lower than 0.25 it means that it is not only the leached sodium that forms formates, but also that there are reactions on the solid catalyst surface forming formates. This is in-line with the DRIFTS results (Fig. 4), where formates are observed on the catalyst surface. However, for the Na/γ-Al_2O_3(27) catalyst, this ratio is close to the theoretical value expected for homogeneous catalysis. This suggests that penta and its derivatives for this specific case could be formed entirely via the Cannizzaro reaction using leached sodium ions into the aqueous phase (Fig. S7b). Conversely, all other catalysts exhibited formaldehyde consumption ratios lower than the theoretical homogeneous case, i.e. lower than 0.25 (Fig. S7b), resulting in that the heterogeneous catalytic sites also must contribute to the Cannizzaro reaction.

The resulting formates then deposited on the catalyst surface, as supported by the DRIFT and TGA analyses of the spent Mg/γ-Al_2O_3(9) catalyst (Fig. 4). Notably, the lowest formaldehyde consumption ratio of

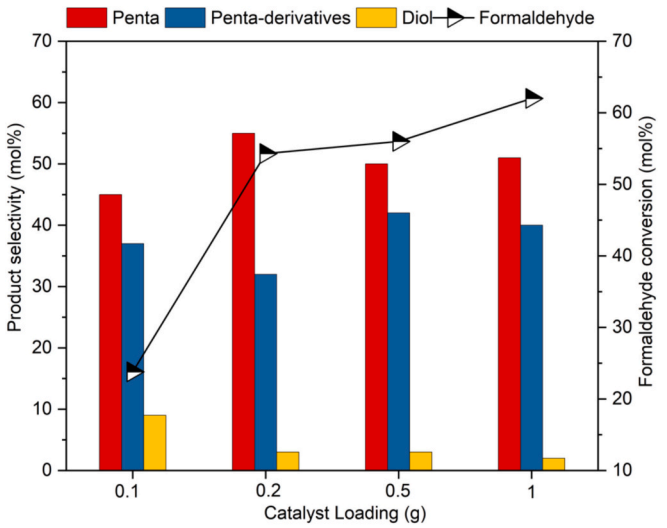

Fig. 7. Mg/γ-Al_2O_3(22) catalysts loading effect on penta synthesis at reaction conditions of formaldehyde to acetaldehyde ratio 5:1 (molar), 15 min reaction time, and at 70 °C temperature. It should be noted that the losses of formaldehyde in blank experiment conducted at 70 °C was 2%, while for acetaldehyde it was 12%.

5×10^{-4} was observed for the Mg/γ-Al_2O_3(9) catalyst, which also showed among the highest selectivity for penta (Fig. 5). This indicates that penta formation with the solid catalysts, especially Mg/γ-Al_2O_3(9), is predominantly driven by heterogeneous basic active sites, although some minor contribution from leached metals cannot be entirely excluded.

3.2.2. Catalyst loading effect

Based on the discussion in Section 3.2.1, Mg/γ-Al_2O_3(22) exhibited high activity for penta synthesis with quite small metal leaching, from 21.5 wt% Mg in fresh catalyst to 17.4 wt% in spent catalyst (after considering the dilution factor 2). To further explore the performance of this catalyst, the effect of catalyst loading on penta synthesis was investigated, as shown in Fig. 7 and Table S6. Increasing the catalyst from 0.1 g to 0.2 g, led to a rise in penta selectivity from 45% to 55%, corresponding to formaldehyde conversions of 24% and 54%, respectively. Moreover, the formation of diol by-products decreased from 9% to 3% with the increased catalyst loading (Fig. 7). However, further increasing the catalyst loading to 0.5 g and 1 g, resulted in an increase in formaldehyde conversion to 56% and 62%, respectively, but also increased selectivity for penta derivatives. Overall, increasing the catalyst amount favored formaldehyde conversion, and selectivity for the sum of penta and penta-derivatives. In general, increasing the catalyst loading accelerated the reactions and advanced the formation of first penta followed by penta-derivatives. The formaldehyde conversion reached a maximum of 62% conversion with 1 g of catalyst and increased from lower loadings (0.2 and 0.5 g). Formaldehyde is initially fed in excess, and this in combination with the measured losses results in that the conversion is limited to 70%. Thus, the conversion did not reach completeness, but it was very high.

Leaching was also examined for these samples, and the results can be found in Fig. S8. Overall, the alkali and alkaline earth metals leaching was between 4-6 percentage points (Eqs. (4)–(5)).

3.2.3. Temperature effect on penta synthesis

Fig. 8 illustrates the effect of temperature on penta synthesis using 0.2 g of Mg/γ-Al_2O_3(22) catalyst, while maintaining the same formaldehyde to acetaldehyde ratio as reported above in Section 3.2.2. In general, formaldehyde conversion increases with temperature from 30 °C to 70 °C, which also impacts the product selectivity due to differences in the activation energies of the reactions. However, when the temperature is raised from 70 °C to 90 °C, the formaldehyde conversion decreases from 54% to 49%. The lower conversion of formaldehyde observed at higher temperatures is most likely caused by increased losses of acetaldehyde at 90 °C, since its high volatility leads to reduced acetaldehyde availability in the reaction mixture, as described in the experimental section. This limited availability of acetaldehyde impacts the condensation reaction and hence the formaldehyde conversion. At 30 °C, only penta and its derivatives were observed, with no diol formation, and a relatively low formaldehyde conversion of 24%. This suggests that diol formation requires a higher activation energy than penta formation and is likely a competing pathway. As the temperature increased to 50 °C, the diol selectivity initially rose, accompanied by a decrease in penta selectivity. At this temperature, selectivity for penta

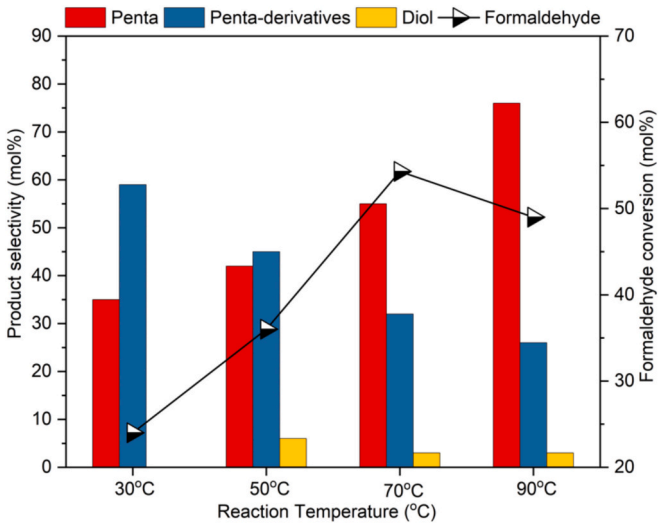

Fig. 8. Temperature effect in the range of 30–90 °C on penta synthesis in the presence of Mg/γ-Al_2O_3(22) catalyst of 0.2 g, and at reaction conditions of formaldehyde to acetaldehyde ratio 5:1 (molar), and 15 min reaction time. It should be noted that the losses of formaldehyde in blank experiment conducted at 70 °C was 2%, while for acetaldehyde it was 12%. The corresponding values at 90 °C was 4 and 62%.

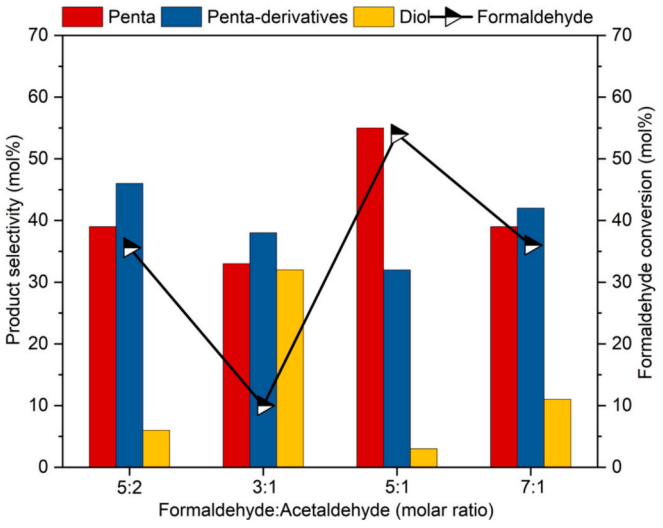

Fig. 9. Formaldehyde to acetaldehyde ratio effect on penta synthesis at reaction conditions of Mg/γ-Al_2O_3(22) catalyst of 0.2 g, 15 min reaction time, and at 70 °C temperature. It should be noted that the losses of formaldehyde in blank experiment conducted at 70 °C was 2%, while for acetaldehyde it was 12%.

and penta-derivatives reached 42% and 45% respectively, with a modest increase in formaldehyde conversion to 36% (Fig. 8 and Table S7). At 70 °C, penta selectivity increased to 55% with 32% selectivity for penta-derivatives, and formaldehyde conversion reached 54%. At 90 °C, penta selectivity increased to 76%, while selectivity for penta-derivatives and diols dropped to 26% and 3%. respectively. These results indicate that selectivity for penta-derivatives decreases with an increase in temperature, suggesting that the activation energy for penta formation is higher than for its subsequent conversion into derivatives. In other words, at elevated temperatures, the initial penta formation proceeds faster than the follow-up reactions forming derivatives. However, Mg metal leaching increased markedly at 90 °C, reaching 12.8 percentage points. After accounting for the dilution factor of 1.4, the Mg content decreased from 21.5 wt% in the fresh catalyst to 8.7 wt% in the spent sample, indicating reduced catalyst stability at elevated temperatures (Fig. S9). The leached metals may also contribute to homogeneous catalysis, potentially altering product selectivity and product distribution in favor of penta formation.

3.2.4. The influence of the reactant ratio on penta synthesis

The influence of changes in the formaldehyde to acetaldehyde molar ratio on penta synthesis was investigated, as shown in Fig. 9 and Table S8. In all previous experiments, a 5:1 M ratio was used, based on literature reports identifying it as an optimized ratio for penta synthesis via homogeneous catalysis [20]. When the formaldehyde to acetaldehyde ratio was altered in the solid catalyst system, significant changes were observed in both penta formation and distribution of side-products. At lower formaldehyde concentrations (both 3:1 and 5:2), the formation of diols and penta-derivatives increased, respectively, as shown in Fig. 9. This suggests that excess acetaldehyde may promote competing condensation reactions and derivatization, leading to diol formation and penta-derivatives. Literature also reports that higher acetaldehyde concentrations favor the formation of penta-derivatives, especially dipenta [39,40]. Among the tested ratios, the 5:2 molar ratio resulted in the highest yield of penta-derivatives with conversion of formaldehyde of 36%. Interestingly, in the case of 5:2 ratio, formaldehyde conversion was high compared to the 3:1 ratio. This effect may be attributed to the formation of penta-derivatives, particularly dipenta and dipenta-derivatives. Because the synthesis of these derivatives requires the generation of acrolein, and acrolein production consumes formaldehyde, the overall formaldehyde conversion increases as a result.

However, at a 3:1 ratio, diol formation dominated, with 32% selectivity, while penta-derivatives reached 38% selectivity. In contrast, the 5:1 ratio, with a modest excess of formaldehyde relative to the stoichiometric requirement for penta formation, was most favorable for driving penta production. This excess formaldehyde also promoted further reactions, converting penta into cyclic penta-derivatives, which reached 32% selectivity. When the ratio was increased to 7:1, the production of penta-derivatives was more similar (39% and 42%, respectively), however the penta selectivity was significantly decreased and the diol formation increased (Table S8).

Moreover, Mg metal leaching during the reactions was measured (Fig. S10). The data showed that the amount of leached metal was quite similar across different molar ratios, indicating that catalyst stability was not significantly affected by changes in reactant ratios.

3.2.5. Reaction time effect

Formaldehyde and acetaldehyde are highly reactive compounds, making it important to examine how reaction time influences product selectivity. Due to their reactivity, product formation begins even during the initial temperature ramping period (ca. 15 min to 70 °C) before the reaction time is reported as 0 min in Fig. 10. At this point, the penta product was already detected. However, formaldehyde conversion was relatively low at 28%. As the reaction time increased to 15 min, under isothermal conditions at 70 °C, the selectivity for penta rose to 55%, while selectivity for penta-derivatives and diols decreased to 32% and 3%, respectively. This shift in selectivity from 0 to 15 min aligns with the temperature-dependent trends shown in Fig. 8. At 70 °C, when increasing the time to 15 min the formation of penta is favored. Beyond 15 min, penta selectivity declined whereas penta-derivatives increased to 52% after 60 min (with 35% penta selectivity), and formaldehyde conversion only weakly continued to increase (Fig. 10 and Table S9). This behavior reflects that the penta derivatives, which are formed from penta, are increasing with time. However, after only heating, this trend is not clear, which might be due to the low formaldehyde conversion. It has been mentioned in the literature that excessive reaction times reduce penta selectivity and yield in favor of its derivatives [18]. The slow increase in formaldehyde conversion beyond 15 min might be due to the deposition of formates — a by-product of the Cannizzaro reaction — on the catalyst surface (Fig. 4), which gradually reduces catalytic activity. Additionally, there are losses of acetaldehyde which would increase with time, further limiting conversion. Hence, an optimum reaction time to achieve high penta selectivity is an important factor. Diol formation

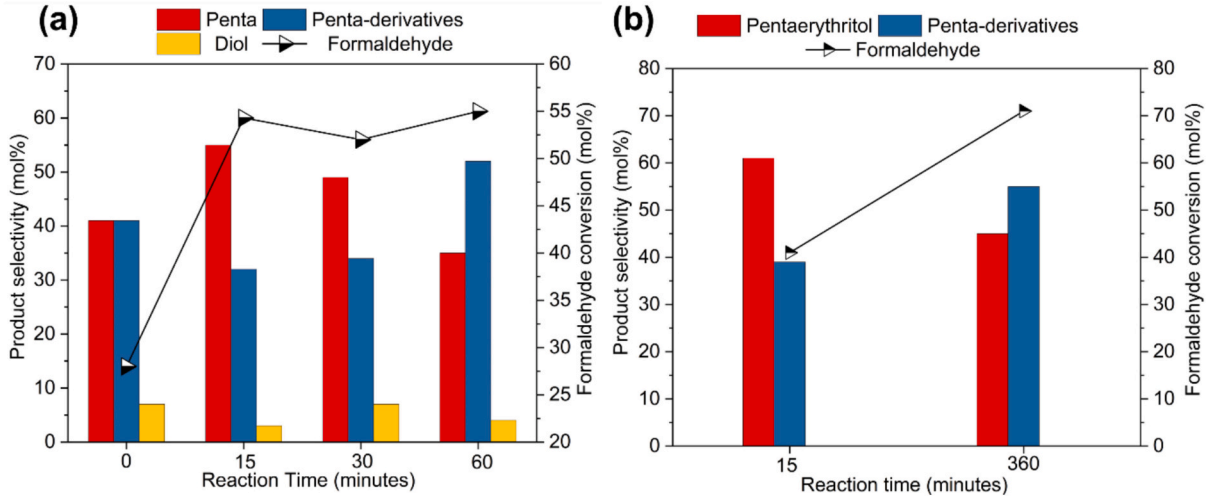

Fig. 10. (a) Reaction time effect from 0 to 60 min on penta synthesis at reaction conditions of Mg/γ-Al_2O_3(22) catalyst (b) of Mg/γ-Al_2O_3(9) for 15 and 360 min. Reaction conditions: catalyst amount of 0.2 g, formaldehyde to acetaldehyde ratio of 5:1 (molar), and at 70 °C temperature. It should be noted that the losses of formaldehyde in blank experiment conducted at 70 °C was 2%, while for acetaldehyde it was 12%.

appears to be fast at the start as a competing reaction, but then penta and penta-derivatives seem to be very dominant as the reaction proceeds for a longer time. Catalyst stability was also evaluated, and ICP analysis of the spent catalysts revealed that Mg metal leaching increased with longer reaction times (Fig. S11). These leached Mg ions dissolved in the aqueous reaction mixture may act as homogeneous catalysts, promoting further reaction of the formed penta with formaldehyde.

A longer reaction time (6 h) was also performed for Mg/γ-Al_2O_3(9) under the same reaction conditions as discussed and the results are shown in Table S9 and can be compared with 15 min for the same catalyst in Table S3. The conversion increased from 41% after 15 min to 71% after 6 h. However, the penta selectivity decreased from 61% to 55% and the penta derivatives increased from 41 to 45%. These results suggests that penta are further transformed to penta derivatives for long reaction time. The conversion was 71% after 6 h, showing that complete conversion was not reached even after 6 h. There is 20% excess of formaldehyde compared to acetaldehyde and the fact that around 12% of the acetaldehyde was lost due to evaporation in blank experiments, results in that the conversion of formaldehyde is maximum ca 70%, which also was the observed conversion. The spent catalyst was examined with TGA (Fig. S12). The weight loss difference between fresh and spent catalyst was 22%, which was the largest weight loss among the spent catalysts obtained after cycling experiments (see Section 3.3). This can be explained by large amount of formates formed on the catalyst after long reaction time. Also, the highest leaching of Mg ions from catalyst surface was observed with 3.7 percentage points after 6 h reaction time (Table S10), compared to 1.5 percentage points for 15 min reaction. This indicated that the stronger interaction of Mg with the support is needed to improve the stability of the catalyst for long run use.

Table 3
BET data for Mg/γ-Al_2O_3(9) catalyst, for fresh, and regenerated (R) and non-regenerated (NR) spent catalysts.

Catalyst	S_{BET} (m^2/g)[a]	V (cm^3/g)[b]	Pore width (nm)
Fresh	93.6	0.418	14.3
Spent, Cycle 1 (NR)	144.7	0.4323	8.9
Spent, Cycle 1 (R)	134.0	0.4447	10.1
Spent Cycle 2 (NR)	153.1	0.3988	7.5
Spent cycle 2 (R)	128.0	0.4571	10.8
Spent cycle 3 (NR)	133.2	0.4137	8.8
Spent cycle 3 (R)	137.3	0.4611	10.4
6 h Spent (NR)	61.4	0.2825	13.1

[a] S_{BET} (total surface area) calculated using the BET equation.
[b] V (total pore volume) calculated by single-point method at $P/P_0 = 0.95$.

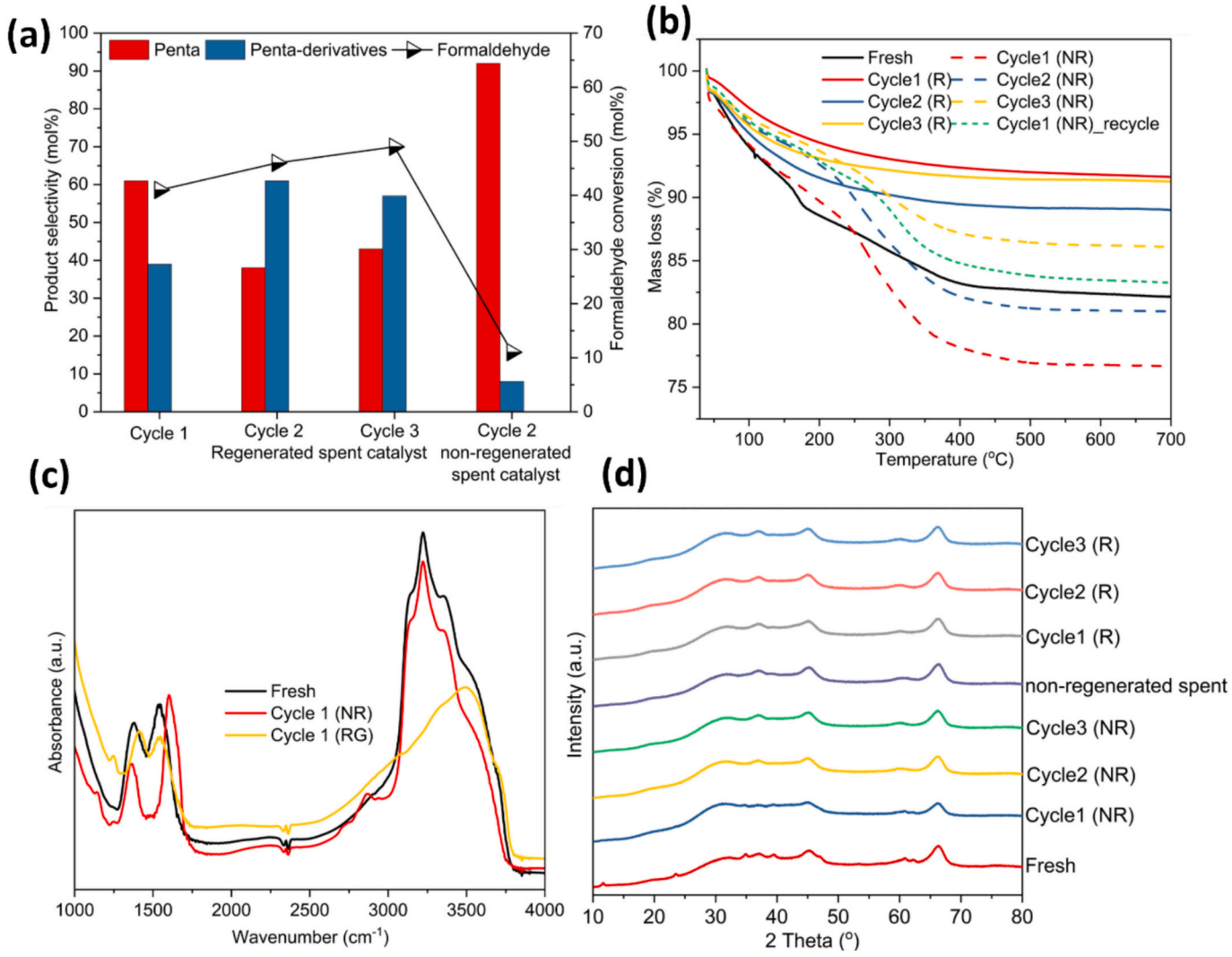

Fig. 11. Mg/γ-Al_2O_3(9) catalyst activity tests in recycling test for penta synthesis at reaction conditions of 0.2 g, formaldehyde to acetaldehyde ratio of 5:1 (molar), 15 min reaction time, and at 70 °C temperature. Results shown for Fresh Cycle 1; Cycle 2 and 3 for regenerated (R) catalyst and Cycle 2 for non-regenerated (NR) catalyst. (a) Activity data, (b) TGA data, (c) DRIFT spectra. It should be noted that the losses of formaldehyde in blank experiment conducted at 70 °C was 2%, while for acetaldehyde it was 12%.

3.3. Catalyst regeneration and recycling

In 1990, Trybula and Terelak [30] compared the conventional alkaline solution, with a solid basic ion exchange resin for penta production. When using the resin, they produced a separate stream of formates in the form of deposits on the catalyst surface, which were separated in post-stream separation steps. The ion exchange resin was regenerated by washing it with NaOH solution and was reused for the penta formation reaction [30]. However, in this reported process, NaOH was still used to regenerate the catalyst which consequently resulted in a stream with formates along with methanol as by-product. In our study, the solid catalyst was regenerated by calcining the spent catalyst and thereafter reusing it for penta formation. Mg/γ-Al_2O_3(9) showed high performance and good stability among the examined catalysts, with no methanol or diol formation, as shown in Fig. 5c. This catalyst was therefore further examined for multiple recycling tests after regenerating the spent catalysts obtained from multiple cycles (Fig. 11).

Firstly, the Mg/γ-Al_2O_3(9) catalyst was separated and dried at 90 °C for 2 h in air, followed by calcination at 450 °C for 1 h in air and named as regenerated spent (Spent R) catalysts. In addition, one spent catalyst was only dried at 90 °C for 2 h and not calcined and this sample is denoted non-regenerated spent catalyst (Spent NR). The activity tests of these regenerated catalysts were performed at reaction conditions of 0.2 g catalyst, formaldehyde to acetaldehyde ratio of 5:1 (molar), 15 min reaction time, and at 70 °C temperature. Interestingly, a slight increase in formaldehyde conversion was observed in both Cycle 2 and Cycle 3 of the regenerated catalysts compared to the fresh catalyst. However, penta selectivity reduced from 61% to 38% and 43% in Cycle 2 and 3, respectively, with an increase in penta-derivatives in both cases (Fig. 11a). This could be linked to the change in structural properties of the regenerated catalysts. An increase in the surface area of both the spent non-regenerated catalyst (NR) and spent regenerated (R) catalysts was observed with a decrease in average pore size, as shown in Table 3. The reason for the increase in surface area compared to the fresh catalyst could be due to leaching of some of the Mg resulting in less pore blocking of Mg. The increase in surface area might provide more active sites to form penta to further derivatize to penta-derivatives, and this could also be the reason that high formaldehyde conversion observed in the recycling tests of the regenerated catalysts. TGA analysis was performed (Fig. 11b), and there was a significant weight loss observed for the spent catalyst for first Cycle for non-regenerated sample, which could be due to large amount of formates and products remaining on the catalyst, which is removed during TGA. However, the TGA for the calcined samples showed less weight loss compared to fresh sample, which could be explained by weight loss during calcination.

To further confirm the results, DRIFT analysis was performed on both non-regenerated and regenerated spent catalysts for Cycle 1, as shown in Fig. 11c. A shift in the peaks was observed in the non-regenerated spent catalyst from 1544 to 1604 cm^{-1} compared to the fresh catalyst. This could be due to formates on the spent catalyst as discussed previously. However, after the regeneration step, the peak around 1604 cm^{-1} disappeared and shifted again to 1544 cm^{-1} as in the case of the fresh catalyst. These results clearly suggest the elimination of formates after the regeneration step, and this can explain why the catalyst activity was partially regained in each cycle test. Moreover, no change in XRD peaks was observed in the regenerated/non-regenerated catalysts obtained from each cycle test (Fig. 11d), suggesting that the crystalline structure was stable for thermal treatment. It should be mentioned that the intensity was slightly decreased for spent catalyst indicating that there might have been some impact on the structure.

The leaching after each cycle was also investigated and is reported as percentage points of Mg obtained from ICP analysis (Table S10) for both fresh and spent catalysts. The leaching of Mg increased for each Cycle, as in Cycle 1, 1.4% points leaching was observed, and in Cycle 2, it was slightly increased to 1.7% points (in comparison to Cycle 1), which was further increased to 2.8% points after Cycle 3. This can be the reason for the decrease in penta selectivity obtained in recycling tests.

Moreover, the non-regenerated spent catalyst obtained after Cycle 1 was also subjected to the catalyst activity test without performing the calcination (regeneration) step, as shown in Fig. 11a. In contrast to the regenerated catalyst cycles, the non-regenerated catalyst exhibited a very high penta selectivity of 92.5%, but this was accompanied by a notably low formaldehyde conversion of only 11.5%. This relatively low yield can be due to the presence of fewer active sites available because of the formate deposition (Fig. 11b and c). Also, this might be the same reason for high penta selectivity, since pores clogged with formates and active sites were covered with residuals from the previous run, which prevents the derivatization reaction from occurring (Table 3). The spent catalyst obtained from this non-regenerated catalyst activity test exhibited larger leaching compared to the regenerated catalyst Cycle 2, with 2.2 percentage points Mg leaching compared to 1.4 percentage points (Table S10). This could be due to the weak bonding of the Mg with the surface due to sharing a bond with deposited formate, which might leave the surface as Mg-formates during the following activity test.

4. Conclusions

Heterogeneous basic catalysts composed of alkali and alkaline earth metals supported on γ-Al_2O_3, SnO_2 and TiO_2 were prepared and evaluated for their activity in producing penta with high selectivity and good formaldehyde conversion. Catalysts containing different alkali and alkaline earth metals, such as Na, Mg, and Ca, on supports exhibited different activities, with the order of effectiveness for penta formation being Mg > Na > Ca. Notably, Mg-based catalysts showed the highest activity and stability during the reaction. Among the tested catalysts, Mg/γ-Al_2O_3(22) demonstrated the best performance at 90 °C, achieving 76% penta selectivity and 49% formaldehyde conversion, however, with large amount of Mg leaching (12.8 percentage points, from 21.5 for fresh catalyst to 8.7 wt% Mg for spent catalyst). Mg/γ-Al_2O_3(9) at 70 °C showed better stability with 1.5 percentage points of Mg leaching (from 9 for fresh catalyst to 7.5 wt% for spent catalyst) and 61% penta selectivity at 41% formaldehyde conversion. Overall, a quite high stability was received with Mg/γ-Al_2O_3(9), with the least amount of Mg leaching ions were the key for efficiently catalyzing penta production, resulting in the best results compared to the other catalysts. In contrast, Na- and Ca-based catalysts exhibited lower penta formation and simultaneously exhibited greater leaching, consequently enhancing their homogeneous catalytic character. However, the deposition of the Cannizzaro by-product formates on the surface of the catalyst, as observed with DRIFT and TGA, can eventually deactivate the catalyst. In multi cycle tests, it was concluded that the regeneration step of the spent catalyst is needed to regain the catalyst performance, however the original activity was not fully regained. This study presents a facile, controlled, and selective route for penta synthesis using a heterogeneous catalyst. It also opens new avenues for further catalyst developments to design more stable catalysts, while maintaining high penta selectivity.

CRediT authorship contribution statement

Aqsa Noreen: Writing – original draft, Methodology, Investigation, Formal analysis, Data curation, Conceptualization. **Abdenour Achour:** Supervision, Methodology. **Oleg Pajalic:** Writing – review & editing, Supervision, Methodology, Funding acquisition, Conceptualization. **Derek Creaser:** Writing – review & editing, Supervision, Methodology, Conceptualization. **Louise Olsson:** Writing – review & editing, Supervision, Project administration, Methodology, Funding acquisition, Conceptualization.

Declaration of competing interest

The authors declare the following financial interests/personal

relationships which may be considered as potential competing interests: Oleg Pajalic reports financial support was provided by Perstorp Specialty Chemicals AB. Oleg Pajalic reports a relationship with Perstorp Specialty Chemicals AB that includes: employment. Louise Olsson is one of the Editors for Chemical Engineering Journal. If there are other authors, they declare that they have no known competing financial interests or personal relationships that could have appeared to influence the work reported in this paper.

Acknowledgements

This project was conducted at the Chemical Engineering division, the Competence Centre for Catalysis (KCK) and the Centre for Process Chemical Engineering (CPE) at Chalmers University of Technology, and was performed in collaboration with Perstorp AB. We gratefully acknowledge the funding from Swedish Energy Agency (P50869-1) and NextGenerationEU (The Recovery and Resilience Facility, RRF). We would like to thank the Chalmers Material Characterization Laboratory (CMAL) for XRD, and SEM access/measurements.

Appendix A. Supplementary data

Supplementary data to this article can be found online at https://doi.org/10.1016/j.cej.2026.177975.

Data availability

Data will be made available on request.

References

[1] B.B. Asare Bediako, Q. Qian, Y. Wang, J. Zhang, Z. Wang, S. Li, H. Liu, T. Wu, M. Ge, B. Han, Synthesis of higher carboxylic acids via reaction of polyols with CO2 and H2, Chem. Catal. 2 (2022) 114–124.
[2] J. Ma, W. Yu, M. Wang, X. Jia, F. Lu, J. Xu, Advances in selective catalytic transformation of ployols to value-added chemicals, Chin. J. Catal. 34 (2013) 492–507.
[3] J. Li, R. Yang, S. Xu, C. Zhou, Y. Xiao, C. Hu, D.C.W. Tsang, Biomass-derived polyols valorization towards glycolic acid production with high atom-economy, Appl. Catal. B Environ. 317 (2022) 121785.
[4] S.S. Saei Dehkordi, J. Albadi, A.A. Jafari, H.A. Samimi, Boric acid/pentaerythritol as a green and reusable catalytic system for the synthesis of mono- and bis-pyrano [2,3-d]pyrimidinone derivatives in water, Polycycl. Aromat. Compd. 43 (5) (2023) 1.
[5] Z. Khademi, K. Nikoofar, F. Shahriyari, Pentaerythritol: a versatile substrate in organic transformations, centralization on the reaction medium, Curr. Org. Synth. 16 (2019) 38–69.
[6] Y. Wang, X. Nie, X. Li, Synthesis and characterization of novel pentaerythritol ester as PVC plasticizer, J. Appl. Polym. Sci. 133 (2016).
[7] A.S. Amarasekara, U. Ha, N.C. Okorie, Renewable polymers: synthesis and characterization of poly(levulinic acid–pentaerythritol), J. Polym. Sci. A Polym. Chem. 56 (2018) 955–958.
[8] L.C. Becker, W.F. Bergfeld, D.V. Belsito, R.A. Hill, C.D. Klaassen, D.C. Liebler, J. G. Marks, R.C. Shank, T.J. Slaga, P.W. Snyder, F.A. Andersen, Safety assessment of pentaerythrityl tetraesters as used in cosmetics, Int. J. Toxicol. 34 (2015) 99S–112S.
[9] R.K. Singh, A. Kukrety, A.K. Singh, Study of novel ecofriendly multifunctional lube additives based on pentaerythritol phenolic ester, ACS Sustain. Chem. Eng. 2 (2014) 1959–1967.
[10] D. Ramos Moreira, M. Worman, E. Nery Ferreira, P. Roberto Campos Flexa Ribeiro Filho, L. Morais Ribeiro da Silva, T. Bezerra Mota Gomes Arruda, F. Eduardo Arruda Rodrigues, F. Murilo Tavares de Luna, C. Liberato Petzhold, M. E. Maier, N. Maria Pontes Silva Ricardo, Development of polyols analogous to neopentyl glycol and trimethylolpropane for the production of oleic acid-based biolubricants, Fuel 381 (2025) 133156.
[11] W.-X. Chen, X.-D. Fan, Y. Huang, Y.-Y. Liu, L. Sun, Synthesis and characterization of a pentaerythritol-based amphiphilic star block copolymer and its application in controlled drug release, React. Funct. Polym. 69 (2009) 97–104.
[12] R. Niu, Z. Zheng, X. Lv, B. He, S. Chen, J. Zhang, Y. Ji, Y. Liu, L. Zheng, Long-chain branched bio-based poly(butylene dodecanedioate) copolyester using pentaerythritol as branching agent: synthesis, thermo-mechanical, and rheological properties, Polymers 15 (2023) 3168.
[13] B. Tang, W. Feng, J. Guo, J. Sun, S. Zhang, X. Gu, H. Li, W. Yang, Hydrophobic modification of pentaerythritol and its application in fire-retardant coatings for steel structures, Prog. Org. Coat. 138 (2020) 105391.
[14] Z. Abd Maurad, S.K. Yeong, Z. Idris, S.A. Ishak, Combined esterification and short-path distillation for high-purity pentaerythritol ester from palm kernel for biolubricants, J. Am. Oil Chem. Soc. 95 (2018) 1421–1429.
[15] A. Noreen, D. Creaser, O. Pajalic, L. Olsson, A review of pentaerythritol synthesis; industrial manufacturing and separation processes, J. Ind. Eng. Chem. 159 (2025) 15.
[16] H.R. Robert, E. John, H. Hasbrouck, Production of Formals of Pentaerythritol, US2464430A, 1949.
[17] T.I. Yoshihiko K, O. Yasuki, Process for Producing Dipentaerythritol, US5254749A, 1991.
[18] M.S. Peters, J.A. Quinn, Pentaerythritol production yields, Ind. Eng. Chem. 47 (1955) 1710–1713.
[19] L.N. Hans B, Process for Producing Monopentaerythritol of High Purity and Monopentaerythritol Produced by the Process, US7569736B2, 2009.
[20] G.R. Owens, Process for Preparation of Pentaerythritol, US40150741A, 1945.
[21] E. Edward A., Acetaldehyde-Formaldehyde Condensation Product, 1941.
[22] W.P.S.L.G. Maury, Conversion of Pentaerythritol Formals Into Pentaerythritol, US2939887A, 1957.
[23] M. Guido Greco, Angelo De Micheli, Umberto Soldano Saronno, Vittorio Bruzzi, Process for Continuous Manufacture of Pentaerythritol, 1965.
[24] L. E., Process for the Preparation of Pentaerythritol, US005741956A, 1998.
[25] X.Y. Yuanhua J, B. Pingguan, F. Jiaxin, D. Jinjun, H. Huazhong, L. Yuanhai, Z. Yexiang, H. Leguan, Method of Preparing Pentaerythritol, US8293950B2, 2006.
[26] D.I. Belkin, O.A. Demchenko, A mathematical model of the synthesis of pentaerythritol, Kinet. Catal. 61 (2020) 374–383.
[27] M. Sluban, B. Cojocaru, V.I. Parvulescu, J. Iskra, R. Cerc Korošec, P. Umek, Protonated titanate nanotubes as solid acid catalyst for aldol condensation, J. Catal. 346 (2017) 161–169.
[28] W. Bing, L. Zheng, S. He, D. Rao, M. Xu, L. Zheng, B. Wang, Y. Wang, M. Wei, Insights on active sites of CaAl-hydrotalcite as a high-performance solid base catalyst toward aldol condensation, ACS Catal. 8 (2018) 656–664.
[29] K.M.A. Santos, E.M. Albuquerque, L.E.P. Borges, M.A. Fraga, Discussing Lewis and Brønsted acidity on continuous pyruvaldehyde Cannizzaro reaction to lactic acid over solid catalysts, Mol. Catal. 458 (2018) 198–205.
[30] S. Trybula, K. Terelak, A Polish process for pentaerythritol manufacture, Pigm. Resin Technol. 19 (1990) 7–8.
[31] Z. Zhang, X. Zhang, L. Zhang, J. Gao, Y. Shao, D. Dong, S. Zhang, Q. Liu, L. Xu, X. Hu, Impacts of alkali or alkaline earth metals addition on reaction intermediates formed in methanation of CO2 over cobalt catalysts, J. Energy Inst. 93 (2020) 1581–1596.
[32] D. Leybo, U.J. Etim, M. Monai, S.R. Bare, Z. Zhong, C. Vogt, Metal–support interactions in metal oxide-supported atomic, cluster, and nanoparticle catalysis, Chem. Soc. Rev. 53 (2024) 10450–10490.
[33] T.M. Rossi, J.C. Campos, M.M.V.M. Souza, CO2 capture by Mg–Al and Zn–Al hydrotalcite-like compounds, Adsorption 22 (2016) 151–158.
[34] H. Hattori, Heterogeneous basic catalysis, Chem. Rev. 95 (1995) 537–558.
[35] O. Kikhtyanin, E. Lesnik, D. Kubička, The occurrence of Cannizzaro reaction over Mg-Al hydrotalcites, Appl. Catal. A Gen. 525 (2016) 215–225.
[36] M. Calatayud, S.E. Collins, M.A. Baltanás, A.L. Bonivardi, Stability of formate species on β-Ga2O3, Phys. Chem. Chem. Phys. 11 (2009) 1397–1405.
[37] T. Moteki, D.W. Flaherty, Mechanistic insight to C–C bond formation and predictive models for cascade reactions among alcohols on Ca- and Sr-hydroxyapatites, ACS Catal. 6 (2016) 4170–4183.
[38] L. Chen, J. Zhao, S.-F. Yin, C.-T. Au, A mini-review on solid superbase catalysts developed in the past two decades, RSC Adv. 3 (2013) 3799–3814.
[39] L. Koudelka, Reactions of acetaldehyde in the preparation of pentaerythntol, Chem. Zvesti. 37 (1983) 374–383.
[40] S.F. Marrian, The chemical reactions of pentaerythritol and its derivatives, Chem. Rev. 43 (1948) 149–202.